Published in final edited form as:
Dev Biol. 2012 May 15; 365(2): 434–444. doi:10.1016/j.ydbio.2012.03.009.

Mutations in vacuolar H+-ATPase subunits lead to biliary developmental defects in zebrafish

Steven F. EauClaire[1], **Shuang Cui**[1], **Liyuan Ma**[1], **James Matous**[1], **Florence L. Marlow**[2], **Tripti Gupta**[2], **Harold A. Burgess**[2], **Elliott W. Abrams**[2], **Lee D. Kapp**[2], **Michael Granato**[2], **Mary C. Mullins**[2], and **Randolph P. Matthews**[1,3,*]

[1]The Children's Hospital of Philadelphia Research Institute, Perelman School of Medicine at the University of Pennsylvania, Philadelphia, PA 19104.

[2]Department of Cell and Developmental Biology, Perelman School of Medicine at the University of Pennsylvania, Philadelphia, PA 19104.

[3]Department of Pediatrics, Perelman School of Medicine at the University of Pennsylvania, Philadelphia, PA 19104.

Summary

We identified three zebrafish mutants with defects in biliary development. One of these mutants, *pekin* (*pn*), also demonstrated generalized hypopigmentation and other defects, including disruption of retinal cell layers, lack of zymogen granules in the pancreas, and dilated Golgi in intestinal epithelial cells. Bile duct cells in *pn* demonstrated an accumulation of electron dense bodies. We determined that the causative defect in *pn* was a splice site mutation in the *atp6ap2* gene that leads to an inframe stop codon. *atp6ap2* encodes a subunit of the vacuolar H^+-ATPase (V-H^+-ATPase), which modulates pH in intracellular compartments. The Atp6ap2 subunit has also been shown to function as an intracellular renin receptor that stimulates fibrogenesis. Here we show that mutants and morphants involving other V-H^+-ATPase subunits also demonstrated developmental biliary defects, but did not demonstrate the inhibition of fibrogenic genes observed in *pn*. The defects in *pn* are reminiscent of those we and others have observed in class C VPS (vacuolar protein sorting) family mutants and morphants, and we report here that knockdown of *atp6ap2* and *vps33b* had an additive negative effect on biliary development. Our findings suggest that pathways important in modulating intracompartmental pH lead to defects in digestive organ development, and support previous studies demonstrating the importance of intracellular sorting pathways in biliary development.

Introduction

Understanding biliary development is vital to determining the pathogenesis of hepatobiliary diseases that affect infants and newborns. Infantile biliary diseases result in cholestasis, or poor bile flow, which may lead to cirrhosis and eventual need for liver transplantation. While only a minority of these conditions has a clear genetic etiology, elucidation of the

*To whom correspondence should be addressed. Randolph P. Matthews, MD, PhD Division of Gastroenterology, Hepatology and Nutrition The Children's Hospital of Philadelphia Research Institute Ph: 267-426-7223 matthews@email.chop.edu.

important genes, proteins, and pathways involved in biliary development will lead to greater understanding of the disease processes and may lead to novel treatments.

We use the zebrafish to model hepatobiliary development and disease. There is generally strong conservation in terms of the overall developmental process and in the importance of specific genetic pathways. In mammals, bipotential hepatoblasts differentiate into hepatocytes and bile duct cells, which form the intrahepatic bile ducts along the developing portal veins, resulting in an arborizing network that drains the liver (Lemaigre and Zaret, 2004). The process of biliary development in mammals continues after birth. In zebrafish, intrahepatic bile ducts lengthen and form connections, leading to a lattice of ducts that drains the liver by around 5 dpf (days post fertilization) (Lorent et al., 2004; Matthews et al., 2004), although the ducts continue to grow and remodel after that time. Mediators of intrahepatic bile duct formation in mammals, such as *Onecut* family members (Clotman et al., 2005; Clotman et al., 2002), the homeodomain transcription factor *Hnf1b* (Coffinier et al., 2002), and *Jagged* and *Notch* (Kodama et al., 2004; Lozier et al., 2008), have generally conserved function in zebrafish biliary development (Lorent et al., 2004; Matthews et al., 2008; Matthews et al., 2004).

Mutagenesis screens in zebrafish allow unbiased discovery of genes important in developmental processes and disease pathogenesis. Numerous investigators have utilized mutagenesis screens to uncover genes involved in gut development (Pack et al., 1996), the effect of maternally expressed genes on early development (Dosch et al., 2004; Wagner et al., 2004), pigment formation (Pickart et al., 2004), and multiple other developmental processes. The fluorescent lipid reporter PED-6 has been utilized in a previous mutagenesis screen to uncover *fat-free* (*ffr*), which demonstrates abnormal lipid processing and defective intrahepatic biliary development (Ho et al., 2006). PED-6 is a quenched phospholipid that is activated by phospholipase A2, absorbed by the enterohepatic circulation, processed by the liver and excreted into intrahepatic bile ducts, and is then excreted into the extrahepatic biliary tree and will accumulate in the gallbladder (Farber et al., 2001). In this study, we used PED-6 to screen for defects in intrahepatic biliary development.

Here we report the identification of three mutants with defects in bile duct development. These mutants -- *pekin* (*pn*), *rouen* (*rou*), and *cayuga* (*cay*) -- are phenotypically distinct. We report that *pn* is caused by a mutation in *atp6ap2*, which encodes an accessory protein to the vacuolar (V)-H^+-ATPase. The V-H^+-ATPase is a multisubunit complex that is critical in lowering pH in lysosomes, endosomes and synaptic vesicles (Forgac, 2007). It also acts at the plasma membrane, lowering extracellular pH within the renal distal tubule (Saroussi and Nelson, 2008). V-H^+-ATPase activity and vesicular acidification are required for normal intracellular vesicular sorting (Mellman et al., 1986; Sun-Wada et al., 2004). Other roles for intravesicular acidification include release and intracellular processing of endocytosed ligands, as well as mediating or preventing viral invasion of cells (Toei et al., 2010). Others have reported zebrafish mutants involving V-H^+-ATPase subunits, which all demonstrate hypopigmentation and share defects in eye development (Amsterdam et al., 2004; Gross et al., 2005; Wang et al., 2008).

Interestingly, in mammals, Atp6ap2 also acts as an intracellular renin receptor that activates ERK1 and ERK2 (Nguyen et al., 2002) and also directly interacts with the transcription factor promyelocytic leukemia zinc finger (PLZF, *Zbtb16*) (Schefe et al., 2006). Prior to the discovery of a distinct renin receptor, renin was known as a protease that activates angiotensin, which upon further modification acts to increase blood pressure by vasoconstriction and by stimulating the release of aldosterone and anti-diuretic hormone. The physiologic actions of the renin receptor (Atp6ap2) overlap some of the effects of renin

itself, including increasing blood pressure (Burckle et al., 2006) and activating fibrosis (Jan Danser et al., 2007).

Our results demonstrate that the V-H^+-ATPase mutant *pn* exhibits developmental biliary defects, most likely via effects on the generation of intracellular pH and vesicular trafficking, and not via effects on renin receptor activity. Knockdown or mutation of genes in intracellular trafficking pathways have been shown previously to lead to abnormal biliary development in zebrafish (Matthews et al., 2005; Sadler et al., 2005; Schonthaler et al., 2008), and patients with a homozygous mutation in the intracellular trafficking gene *VPS33B* develop severe cholestasis (Gissen et al., 2004). These findings, along with those presented here, stress the importance of intracellular trafficking pathways in biliary development and disease pathogenesis.

Materials and methods

Mutagenesis screen for biliary defects

A chemical mutagenesis screen using ethylnitrosourea (ENU) was performed essentially as described previously (Dosch et al., 2004; Wagner et al., 2004), screening the equivalent of 600 genomes. We used PED-6 to screen for families in which ¼ of the F3 members demonstrated diminished gallbladder uptake, similar to previous (Farber et al., 2001; Ho et al., 2006). PED-6 is a fluorescent lipid compound that is activated in the intestine and absorbed via the enterohepatic circulation into the liver, where it is processed in the hepatocyte and excreted into the bile, accumulating in the gallbladder (Farber et al., 2001). Lack of gallbladder accumulation suggests possible abnormalities in intrahepatic biliary development. All fish were cared for in the zebrafish facility at the University of Pennsylvania or The Children's Hospital of Philadelphia Research Institute, in accordance with Institutional Animal Care and Use Committee guidelines of both institutions.

Genetic identification of *pn* was performed on F2 progeny, to take advantage of the generation of mutant carriers in AB/Tü strain hybrids. A large panel of standard z-markers was used to establish linkage on chromosome 22, and finer mapping was performed using primers listed in Supplemental Table 1. Candidate genes were identified based on available sequence data (www.sanger.ac.uk) and sequenced using primers designed on the available *in silico* sequence. Screening for carrier heterozygotes was performed using TaqMan primers containing the single nucleotide polymorphism (SNP) constituting the mutation (Table S1). The altered transcript in the mutant was confirmed using standard and quantitative PCR, with primers shown in Table S1.

Additional mutant lines were obtained from the zebrafish international resource center (ZIRC). These lines were originally uncovered in an insertional mutagenesis screen in the Hopkins laboratory (Amsterdam et al., 1999). The lines included hi3681 (*atp6ap2*), hi112 (*atp6ap1*), and hi2188b (*atp6v0d1*). In addition, we used morpholinos directed against *atp6v1a* (Supplemental Table 2) to establish additional models of V-H^+-ATPase subunit mutants.

In situ hybridization

In situ hybridizations were performed as described previously (Cui et al., 2011a), except that 0.25% acetic anhydride was added after proteinase K fixation to reduce background (Westerfield, 2000). Primers for synthesis of the *foxa3, atp6ap2* and *dct* probes are noted in Table S2. As a control, larvae with no riboprobe added were processed identically to the samples with riboprobes.

Tissue histology and immunostaining

For experiments involving conventional stainings such as hematoxylin and eosin, 5 dpf larvae were fixed in 4% paraformaldehyde, embedded in paraffin, and sectioned. Slides were treated as per standard protocol and then stained with hematoxylin and eosin. Staining for Atp6ap2 was performed on unstained sections from wild-type 5 dpf larvae in accordance to standard techniques, using an antibody against the renin receptor (H-85; sc-67390; Santa Cruz Biotechnology). As a negative control, sections were treated using the same protocol but without primary antibody.

Whole-mount cytokeratin and 2F11 staining were performed as previously described, after fixation in methanol/DMSO or paraformaldehyde (Matthews et al., 2008). Duct quantification was performed identically to previous (Cui et al., 2011a).

Electron microscopy

Samples for electron microscopy were obtained at 5 dpf. Larvae were fixed in buffered glutaraldehyde and prepared as previously (Matthews et al., 2005). Sections were examined at the Penn Bio-Imaging Core, as previously.

Non-quantitative PCR and quantitative real-time PCR

Samples for examination of *atp6ap2* expression were obtained by dissecting the liver out of 5 dpf larvae. RNA was isolated from the liver and from separate whole wild-type larva in pooled batches of 5 larvae, reverse transcribed and PCR was performed with primers shown in Supplemental Table 3.

Samples for quantitative real-time PCR were obtained at 5 dpf. RNA was isolated from whole larvae and was reverse transcribed as per standard protocols, and QPCR was performed generally in accordance with standard protocols, using a StepOne Plus from ABI. Primers are depicted in Supplemental Table 3. Normalization was performed using *hprt*. Graphs depicted are representative experiments comparing 4 individual biological replicates per condition, in quadruplicate.

Morpholino injections

Morpholinos to *vps33b, atp6ap2, atp6v1a* and *ren* were obtained from Gene-Tools (Philomath, OR). Sequences of the *atp6ap2, atp6v1a* and *ren* MOs are depicted in Table S2. Morpholinos were injected at the one-cell stage, similar to previous, and titrated to effect. We have previously demonstrated functionality and specificity of the *vps33b* MOs (Matthews et al., 2005). Quantitative PCR documentation of the effect of *atp6v1a* is shown in Figure S1.

Results

Screen for developmental biliary defects

We participated in a multi-investigator ENU mutagenesis screen, similar to previous studies (Dosch et al., 2004; Wagner et al., 2004). We screened F3 families for biliary defects using the fluorescent lipid reporter PED-6, which has previously been used as a screening tool for developmental biliary defects in zebrafish (Farber et al., 2001; Ho et al., 2006). We identified several F3 families with distinct abnormalities in gallbladder PED-6 accumulation, of which we present the initial characterization of three. The general appearance of and lack of gallbladder PED-6 in the mutants *pekin* (*pn*), *rouen* (*rou*), and *cayuga* (*cay*) are depicted in Figure 1. Of these mutants, *pn* was also notable for generalized hypopigmentation, and *rou* demonstrated cardiac edema. All three mutants demonstrated

smaller eyes and an underinflated swim bladder, and *pn* and *rou* demonstrated underutilized yolk. The lack of gallbladder PED-6 in these mutants suggested possible defects in biliary development.

Mutants with intrahepatic biliary defects

We examined *pn, rou*, and *cay* for defects in intrahepatic biliary development using whole-mount cytokeratin immunostaining of liver from 5 dpf larvae, similar to previous studies (Ho et al., 2006; Lorent et al., 2004; Matthews et al., 2008; Matthews et al., 2004; Matthews et al., 2005). All three mutants demonstrated distinct and severe defects of intrahepatic biliary anatomy at 5 dpf when compared to wild-type (Figure 2). The staining pattern in *pn* demonstrated a similar number of ducts as seen in wild-type, but shorter and wider, with a modest decrease in the interconnecting ducts and terminal ductules that appear later in development (Fig. 2 and Table 1). In contrast, *rou* livers appeared even more abnormal, with significantly fewer ducts almost devoid of interconnecting ducts and terminal ductules. The ductal network of *cay* appeared to have fewer ducts than wild-type but the ducts were of a similar length, although *cay* ducts also demonstrated decreased numbers of interconnecting ducts and terminal ductules. These patterns are schematized in Figure 2 and quantified in Table 1. We also examined our mutants using the bile duct cell marker 2F11 (Crosnier et al., 2005). Using this marker, *pn* appeared to have smaller bile duct cell bodies, *rou* was devoid of bile duct cells, and *cay* was difficult to distinguish from wild-type (Fig. 2).

Ultrastructural examination of the mutants demonstrated distinct findings as well. As depicted in Figure 2, bile duct cells in *pn* demonstrated accumulation of electron dense bodies at the periphery of the cell, with an accumulation of vesicles or dilation of the smooth endoplasmic reticulum as well. As depicted in the inset (Figure 2N'), the electron dense bodies appeared striped, resembling "zebra bodies", which have been described in patients with lysosomal storage diseases (Aleu et al., 1965). Along with the dilated vesicular structures, this suggested that there might be a defect in protein targeting or degradation in *pn*. We were unable to find bile duct cells in *rou* by electron microscopy, consistent with the cytokeratin and 2F11 immunostainings, and areas in the liver that normally contain bile duct cells were occupied by large cells, probably macrophages, with multiple structures within (Fig. 2O). The continued presence of apparent cytokeratin staining at 5 dpf without evidence for bile duct cells at that stage could be due to remnants of ductal structures that appeared earlier, suggesting that *rou* mutation may lead to degradation of bile duct cells. The ultrastructural defects of *cay* appeared subtle, as the nuclei of the bile duct cells appeared mildly enlarged relative to the cytoplasm and the bile duct cells themselves appeared somewhat more similar to the hepatocytes (Fig. 2P). These results demonstrate that the intrahepatic biliary defects in *pn, rou*, and *cay* are distinct.

The zebrafish mutant pn and atp6ap2

Genetic characterization of *pn* demonstrated a mutation in the intron-exon boundary at the end of the 8th exon of the gene *atp6ap2*, c.980+2T->G, resulting in a read-through and premature stop codon (Figure 3). No mutations were detected in the neighboring genes depicted in Figure 3. Semi-quantitative PCR of *pn* cDNA demonstrated the presence of a larger band corresponding to the alternate splice product (Figure 3B), confirmed by sequence analysis, which is dramatically increased in *pn* (Figure 3C). Successful non-complementation using the *atp6ap2* insertional mutant *hi3681* confirmed that the causative gene of *pn* is *atp6ap2*. Of note, phenotypic analysis of *hi3681* was indistinguishable from *pn* (data not shown). Injection of morpholino antisense oligonucleotides directed against the *atp6ap2* translational start site, splice acceptor site of exon 2, or splice donor site of exon 8 led to diminished gallbladder uptake and abnormal intrahepatic ducts similar to *pn* (data not shown). The *atp6ap2* gene was ubiquitously expressed at low levels throughout the

developing embryo and larva, including the developing liver at 3 dpf (data not shown and www.zfin.org). At 5 dpf, *atp6ap2* was expressed relatively faintly in the liver, as well as in mucus cells in the skin, as determined by *in situ* hybridization and by PCR from livers isolated from 5 dpf larvae (Figure 3). Immunostaining demonstrated punctate staining consistent with vesicular localization in 5 dpf digestive organs (Figure 3). These findings demonstrate that the causative gene of *pn* is a mutation in *atp6ap2*, thus suggesting that a mutation in *atp6ap2* leads to the biliary phenotype of *pn*. Interestingly, similar low levels of expression were noted of *cog8*, the causative gene of *ffr* (Ho et al., 2006). Genetic analysis of *rou* and *cay* is ongoing.

The hypopigmentation found in other zebrafish V-H^+-ATPase mutants (Amsterdam et al., 2004; Gross et al., 2005; Wang et al., 2008) supports a role for Atp6ap2 in V-H^+-ATPase activity. Decreased Atp6ap2 activity in *pn* would be expected to inhibit V-H^+-ATPase activity, affecting intracompartmental pH. As mentioned above, the V-H^+-ATPase has numerous effects and thus an inability to lower intracompartmental pH could have effects on ligand processing, intracellular sorting, degradation of proteins in the lysosomes, or other effects. Atp6ap2 also acts as an intracellular renin receptor, with downstream effects on ERK and the transcription factor PLZF. Consistent with previous reports, *pn* larvae demonstrated decreased expression of *pik3r* (Figure 3), a downstream target of PLZF (Schefe et al., 2006) that encodes the p85α subunit of phosphoinositol-3-kinase. These findings suggest that at least some of the functions of Atp6ap2, including effects on PLZF targets and skin hypopigmentation, are conserved in zebrafish.

We have uncovered a mutation in a gene encoding a protein with two roles: modulation of V-H^+-ATPase activity and intracellular renin receptor. Modulation of V-H^+-ATPase activity will lead to a decreased ability to acidify intracellular compartments, and thus could have an effect on protein degradation or trafficking consistent with the defects noted in *pn* biliary cells by ultrastructure. We hypothesized that the Atp6ap2 effects on V-H^+-ATPase activity, and not the effects mediated as the renin receptor, led to the biliary defects. We were also interested in other defects in *pn*, to determine the effects of mutation of *atp6ap2* on other tissues.

Additional defects in pn

Genetic identification of *atp6ap2* as the causative gene in *pn* allowed us to examine *pn* in greater depth. We examined *pn* larvae at 4 dpf to determine the extent of the intrahepatic biliary defects at that stage. Previous work has demonstrated that in the initial stages of intrahepatic biliary development, scattered ducts lengthen and then become interconnected, with the terminal ductules, or anastamoses with hepatocyte canaliculi, appearing while these interconnections are being made (Lorent et al., 2010; Lorent et al., 2004; Matthews et al., 2004). Defects in intrahepatic biliary anatomy in *pn* were severe at 4 dpf, with shorter ducts and a lack of interconnecting ducts and terminal ductules (Figure 4), similar to the phenotype at 5 dpf. The pattern of intrahepatic ducts in *pn* at 4 and 5 dpf suggested that the development of intrahepatic bile ducts in *pn* is relatively specific, especially when compared to the overall normal appearing liver at 5 dpf by hematoxylin and eosin staining (Figure 4E-F). This suggests that liver defects in *pn* are defects in either bile duct formation or on the biliary cells themselves, based on the abnormal appearance of these cells by ultrastructure (Figure 2M-N).

The ultrastructural appearance of bile duct cells in *pn* suggested defects in protein trafficking or impairment in protein degradation, which is consistent with the previously described effects of inhibition of the V-H^+-ATPase. Hypopigmentation, as seen in *pn*, is a common phenotype in other V-H^+-ATPase mutants. We were unable to find melanocytes in 5 dpf *pn* larvae (data not shown), and there was decreased expression of the melanoblast marker *dct*

at 5 dpf by qPCR, although melanoblast expression of *dct* appeared normal at 24 hpf (Supplemental Figure 2), suggesting that melanocytes are forming properly but degrade. Because *pn* eyes also appeared hypopigmented, we examined eye anatomy at 5 dpf. Cell layers within the eye were disrupted in *pn* (Figure 3G-H), with the most striking abnormalities in the retinal cell layer and the retinal pigmented epithelium. These findings are similar to previous descriptions of eye pigmentation mutants caused by mutations in genes encoding subunits of the V-H^+-ATPase and vacuolar protein sorting (VPS) complexes (Navarro et al., 2008), complexes important in intracellular protein trafficking and degradation.

We examined other digestive tissues for abnormalities similar to those caused by defects in other trafficking genes, such as *ffr*, in which there is a mutation in the Golgi protein Ffr/Ang2 and there are defects in both exocrine pancreas and in intestinal ultrastructure (Ho et al., 2006). Examination of expression of the early digestive organ marker *foxa3* in *atp6ap2* morphants at 36 hpf demonstrated no abnormalities (Supplemental Figure 3), suggesting that early gut development is not affected by inhibition of *atp6ap2*. There were no zymogen granules in the pancreas of 5 dpf *pn* larvae (Figure 4I-J), and close examination of *pn* enterocytes demonstrated dilated Golgi (Figure 4K-L). These findings were similar to defects found in *ffr*, which also demonstrate abnormal bile duct morphology (Ho et al., 2006). The biliary and pancreatic defects in *pn* are more severe when compared to *ffr*, however, and *ffr* larvae are normally pigmented. Thus, *pn* phenotypes involving hypopigmentation of the skin and eye, as well as digestive organ abnormalities also observed in other trafficking mutants strongly suggest that trafficking defects lead to the *pn* phenotype. Skin hypopigmentation, lack of zymogen granules, and the presence of electron dense material in biliary cells are distinct findings that we and others have not seen previously in several mutants and morphants with biliary developmental defects (Cui et al., 2011a; Cui et al., 2011b; Lorent et al., 2004; Matthews et al., 2011; Matthews et al., 2009; Matthews et al., 2008; Matthews et al., 2004; Sadler et al., 2005; Yee et al., 2005).

Biliary defects in other V-H^+-ATPase subunit mutants

Atp6ap2 mediates the function of V-H^+-ATPase, and also transmits signals through ERK and through transcription factors such as PLZF. To determine whether inhibition of V-H^+-ATPase activity leads to biliary defects, we examined other V-H^+-ATPase mutants for abnormalities in biliary development. The ability to transmit signals through ERK and PLZF appears to be unique to Atp6ap2 and its role as the intracellular renin receptor. Thus, developmental biliary defects in multiple V-H^+-ATPase mutants would suggest that these defects are due to abnormalities in vesicular acidification.

In addition to *pn*, there are several zebrafish lines in which there is a mutation in a subunit of the V-H^+-ATPase, including *atp6v0d1, atp6ap1* and others. These mutants were uncovered as part of a large insertional mutagenesis screen (Amsterdam et al., 1999). Gallbladder PED-6 uptake in *atp6v0d1* and *atp6ap1* mutants and in *atp6v1a* morphants was diminished, similar to *pn* (Figure 5). As depicted in Figure 5 and Table 1, cytokeratin immunostaining of whole-mount liver from 5 dpf *atp6v0d1*$^{-/-}$, *atp6ap1*$^{-/-}$, and *atp6v1a* morphant larvae demonstrated a decrease in the number and complexity of intrahepatic ducts, similar to *pn*. Of note, knockdown of *ren* (renin) led to minor defects in biliary development difficult to distinguish from control and less significant than defects in *pn* and other V-H^+-ATPase mutants and morphants (supplemental Figure 4). These results are consistent with a role for V-H^+-ATPase and an importance of intracellular vesicular acidification in zebrafish biliary development.

Examination of fibrogenic gene expression changes in pn and other V-H$^+$-ATPase mutants

As mentioned above, in addition to the effects on V-H$^+$-ATPase activity, Atp6ap2 mediates effects via ERK and PLZF after activation by renin. The effects leading to hypopigmentation and biliary development appear to be shared with at least three other V-H$^+$-ATPase subunit genes (Figure 5). Downstream effects of renin via the renin receptor include stimulatory effects on fibrogenesis, and thus fibrogenic gene expression changes might be mediated via PLZF or ERK. We examined fibrogenic gene expression changes in *pn* as a marker of Atp6ap2 activity independent of V-H$^+$-ATPase effects. As depicted in Figure 6, there was a decrease in early markers of fibrosis such as *hsp47* (Masuda et al., 1994), *vime*, and *col1a1* in *pn*, suggesting that the fibrogenesis pathway is inhibited in *pn*. Similar results were obtained in *hi3681* mutants and in *atp6ap2* morphants (data not shown). In contrast, there was no change in expression of these genes in *atp6v0d1* or *atp6ap1* mutants, or in *atp6v1a* morphants, while there was a significant decrease in expression in *ren* morphants (Supplemental Figure 5). These findings, along with demonstration that *ren* knockdown has no effect on biliary development (Fig. S4), suggest that the effects of Atp6ap2 on biliary development and involving changes in fibrogenic gene expression are separable, and supports a more important role for the effects on V-H$^+$-ATPase activity leading to the biliary defects. Thus, intracellular compartmental pH regulation appears more important in mediating biliary development, as opposed to the renin receptor function of Atp6ap2.

Inhibition of atp6ap2 and vps33b affects biliary development

We and others have demonstrated the importance of genes in intracellular trafficking and sorting pathways in zebrafish intrahepatic biliary development, as mutation or knockdown of *vps33b, vps18*, and *vps39* leads to abnormal biliary development (Matthews et al., 2005; Sadler et al., 2005; Schonthaler et al., 2008). These genes encode proteins important in the docking of membrane vesicles, in particular in mediating the progression of late endosomes to lysosomes. Given the importance of low pH in lysosome function, we hypothesized that *atp6ap2* and other V-H+-ATPase genes might be mediating a similar effect on intrahepatic biliary development. Thus, we performed morpholino-mediated knockdown experiments using morpholinos against *vps33b* and *atp6ap2*. Similar to previous experiments, we injected morpholinos at concentrations that alone produced only a mild effect. As demonstrated in Figure 7, when combined, injection of the morpholinos at the lower amounts led to abnormal intrahepatic biliary development, suggesting that the two genes are functioning in the same pathway at some level. Figure 7 also demonstrates that the effect on development of either morpholino alone at lower concentrations is in fact mild, while together they exert an effect similar to that seen in *pn*. This suggests that VPS-mediated effects and V-H$^+$-ATPase-mediated effects converge, possibly on the same intracellular compartment or both affecting transport of a critical mediator, and that inhibition of this function leads to abnormal intrahepatic biliary development.

Discussion

Here we have presented three novel zebrafish mutants with developmental biliary defects. One of these mutants, *pn*, is caused by mutation of the *atp6ap2* gene, which encodes a protein that acts as part of the V-H$^+$-ATPase complex. This complex has been shown to modulate pH in intracellular vesicles, and the Atp6ap2 subunit has been shown to have an additional role as an intracellular renin receptor. Several zebrafish mutants and morphants of genes shown to be important in intracellular trafficking are associated with intrahepatic biliary defects, and we demonstrate that knockdown of *atp6ap2* is additive with knockdown of *vps33b*. These results suggest that in zebrafish, inhibition of pathways important in

intracellular trafficking and in protein degradation negatively affects intrahepatic biliary development.

The three mutants reported here that were uncovered by screening with the lipid reporter PED-6 support this as a useful screening method. Previously, *ffr* was uncovered by PED-6, and additional mutants from this screen will be reported elsewhere. Each of the mutants reported here appears distinct, with different overall appearance and different cytokeratin patterns and ultrastructural appearance. Thus, further mutants could be uncovered by this method, as we do not appear to have reached saturation. Certainly our method of screening for biliary defects at 5 dpf will not uncover mutants in genes affecting vital early processes, as those mutants are not likely to be viable at 5 dpf. Thus, our screen selects for genes that do not have an additional function that is vital in the early embryo. Interestingly, to date this has resulted in the uncovering of two genes shown to have roles associated with intracellular trafficking, in *ffr* and *pn*.

Intracellular trafficking pathways and biliary development

This report represents the fifth example of a zebrafish mutant or morphant in which presumed defects in intracellular trafficking, broadly defined, are associated with developmental biliary defects. Others include *ffr, vps18* and *vps39* mutants and *vps33b* morphants. These models share other defects, including intestinal and pancreatic abnormalities and hypopigmentation (although not all of these models demonstrate all of these phenotypes), which are not seen in other zebrafish biliary mutants. The gene affected in *ffr* encodes a COG family protein; the COG complex has been shown to be important in mediating vesicular transport to, from and within the Golgi in yeast and in mammalian cells (Oka and Krieger, 2005). VPS18, VPS39 and VPS33B are vacuolar sorting proteins that mediate trafficking between late endosomes and lysosomes in multiple model systems ranging from yeast and plants to mammals (Nickerson et al., 2009). As stated above, the V-H^+-ATPase complex has been shown to be important in acidifying intracellular vesicles, including late endosomes and lysosomes, in multiple model systems including yeast (Forgac, 2000), Drosophila (Yan et al., 2009), fish (Kern et al., 2002) and mammalian (Nakamura et al., 1997) cell culture, and others. Zebrafish models affecting these complexes likely disrupt intracellular trafficking pathways, leading to abnormal protein targeting and/or degradation.

Several liver diseases result from mistargeting of proteins, although the primary defect in these diseases is not a defect in the trafficking pathway. Alpha-1-antitrypsin deficiency results in the accumulation of alpha-1-antitrypsin in the endoplasmic reticulum, leading to liver disease (Carlton et al., 2004). Patients with cystic fibrosis may have mistargeting of the cystic fibrosis transmembrane conductance regulator (CFTR) that results in liver damage (Feranchak and Sokol, 2001), while those with progressive familial intrahepatic cholestasis (PFIC) syndromes have mutations in specific bile component transporters that result in a lack of protein or impaired transport to the hepatocyte plasma membrane (Carlton et al., 2004). Thus, disorders in which proteins are mistargeted lead to biliary defects, although these defects do not seem to be developmental.

With respect to *pn* and other mutants and morphants with defects in pathways affecting late endosomes and lysosomes, defects may arise from accumulation of cytotoxic proteins and/or abnormal trafficking of proteins important in biliary development. Specific mediators of biliary development such as Jagged/Notch and TGFβ may be affected, as vesicular acidification and intracellular trafficking are important in the activity for both signaling pathways. Jagged and Notch family members have clearly been implicated in biliary development in mammals and zebrafish (Loomes et al., 2007; Lorent et al., 2004; Ryan et al., 2008; Zong et al., 2009), and TGFβ plays a role in biliary development through

interaction with Hnf6 activity (Clotman et al., 2005) and possibly an effect on Notch target genes (Blokzijl et al., 2003). Both Jagged and Notch undergo endocytosis to initiate and terminate signaling between adjacent cells (Nichols et al., 2007), and proteolytic cleavage of Notch is critical at several steps in activation (Kadesch, 2004). Acidification of TGFβ leads to activation and release from intracellular vesicles (Gleizes et al., 1997; Roth-Eichhorn et al., 1998), and the endocytic internalization of the TGFβ receptor is required for signaling (Le Roy and Wrana, 2005). The requirement for both Jagged/Notch and TGFβ signaling suggests possible mechanisms by which abnormal intracellular trafficking could lead to developmental biliary defects. Alternatively, impaired degradation of proteins in biliary cells could lead to the effects as well.

Mutations in V-H^+-ATPase genes would be expected to cause abnormalities in intravesicular acidification. While no liver diseases specifically attributed to impaired organelle acidification have been described, disorders of organelles in which establishment of low pH is critical, such as lysosomes, are important causes of liver disease. Infants with lysosomal storage diseases such as Niemann-Pick C and Gaucher disease present with cholestasis, suggesting that abnormal intracompartmental pH, as would be generated by V-H^+-ATPase defects, can result in infantile cholestatic disorders. Again, these disorders do not appear to be developmental in etiology, but their occurrence during infancy, when intrahepatic bile ducts continue to be remodeled, suggests that there may be an impact on developmental processes.

We and others have demonstrated an association between inhibition of trafficking genes and a phenotype involving skin and eye hypopigmentation, developmental biliary defects, and defects in organelles involved in intracellular trafficking in other digestive tissues. While this association suggests an importance of these genes in the affected processes, the effect may be indirect, and we cannot exclude the possibility that the observed phenotypes may be the result of some other effect of inhibition of trafficking genes. One possible alternative would be an effect of these proteins on cell polarity pathways, including planar cell polarity, which we have recently shown plays an important role in biliary morphogenesis (Cui et al., 2011a).

We have presented mutants affecting biliary development in zebrafish, including another example of a mutant in which an intracellular trafficking pathway is impaired. Continued analysis of these mutants and others will likely uncover genes and pathways not previously appreciated as important in biliary development. These mutants also provide further models of biliary defects, which should allow greater understanding of such defects in patients.

Supplementary Material

Refer to Web version on PubMed Central for supplementary material.

Acknowledgments

The authors thank Drs. Michael Pack and Kristin Lorent for advice and helpful discussions. We also thank Ashley Edens for expert technical assistance, and Drs. Pierre Russo and Neleema Shah for help in interpretation of electron micrographs. This work was supported by the NIH (K08 DK068009, R03 DK080710 to R.P.M.; R01 HD050901 to M.M.), as well as institutional support from The Children's Hospital of Philadelphia and the Fred and Suzanne Biesecker Pediatric Liver Center.

References

Aleu FP, Terry RD, Zellweger H. Electron Microscopy of Two Cerebral Biopsies in Gargoylism. J Neuropathol Exp Neurol. 1965; 24:304–17. [PubMed: 14280504]

Amsterdam A, Burgess S, Golling G, Chen W, Sun Z, Townsend K, Farrington S, Haldi M, Hopkins N. A large-scale insertional mutagenesis screen in zebrafish. Genes Dev. 1999; 13:2713–24. [PubMed: 10541557]

Amsterdam A, Nissen RM, Sun Z, Swindell EC, Farrington S, Hopkins N. Identification of 315 genes essential for early zebrafish development. Proc Natl Acad Sci U S A. 2004; 101:12792–7. [PubMed: 15256591]

Blokzijl A, Dahlqvist C, Reissmann E, Falk A, Moliner A, Lendahl U, Ibanez CF. Cross-talk between the Notch and TGF-beta signaling pathways mediated by interaction of the Notch intracellular domain with Smad3. J Cell Biol. 2003; 163:723–8. [PubMed: 14638857]

Burckle CA, Jan Danser AH, Muller DN, Garrelds IM, Gasc JM, Popova E, Plehm R, Peters J, Bader M, Nguyen G. Elevated blood pressure and heart rate in human renin receptor transgenic rats. Hypertension. 2006; 47:552–6. [PubMed: 16401765]

Carlton VE, Pawlikowska L, Bull LN. Molecular basis of intrahepatic cholestasis. Ann Med. 2004; 36:606–17. [PubMed: 15768832]

Clotman F, Jacquemin P, Plumb-Rudewiez N, Pierreux CE, Van der Smissen P, Dietz HC, Courtoy PJ, Rousseau GG, Lemaigre FP. Control of liver cell fate decision by a gradient of TGF beta signaling modulated by Onecut transcription factors. Genes Dev. 2005; 19:1849–54. [PubMed: 16103213]

Clotman F, Lannoy VJ, Reber M, Cereghini S, Cassiman D, Jacquemin P, Roskams T, Rousseau GG, Lemaigre FP. The onecut transcription factor HNF6 is required for normal development of the biliary tract. Development. 2002; 129:1819–28. [PubMed: 11934848]

Coffinier C, Gresh L, Fiette L, Tronche F, Schutz G, Babinet C, Pontoglio M, Yaniv M, Barra J. Bile system morphogenesis defects and liver dysfunction upon targeted deletion of HNF1beta. Development. 2002; 129:1829–38. [PubMed: 11934849]

Crosnier C, Vargesson N, Gschmeissner S, Ariza-McNaughton L, Morrison A, Lewis J. Delta-Notch signalling controls commitment to a secretory fate in the zebrafish intestine. Development. 2005; 132:1093–104. [PubMed: 15689380]

Cui S, Capecci LM, Matthews RP. Disruption of planar cell polarity activity leads to developmental biliary defects. Dev Biol. 2011a; 351:229–41. [PubMed: 21215262]

Cui S, Erlichman J, Russo P, Haber BA, Matthews RP. Intrahepatic Biliary Anomalies in a Patient With Mowat-Wilson Syndrome Uncover a Role for the Zinc Finger Homeobox Gene zfhx1b in Vertebrate Biliary Development. J Pediatr Gastroenterol Nutr. 2011b; 52:339–44. [PubMed: 21336163]

Dosch R, Wagner DS, Mintzer KA, Runke G, Wiemelt AP, Mullins MC. Maternal control of vertebrate development before the midblastula transition: mutants from the zebrafish I. Dev Cell. 2004; 6:771–80. [PubMed: 15177026]

Farber SA, Pack M, Ho SY, Johnson ID, Wagner DS, Dosch R, Mullins MC, Hendrickson HS, Hendrickson EK, Halpern ME. Genetic analysis of digestive physiology using fluorescent phospholipid reporters. Science. 2001; 292:1385–8. [PubMed: 11359013]

Feranchak AP, Sokol RJ. Cholangiocyte biology and cystic fibrosis liver disease. Semin Liver Dis. 2001; 21:471–88. [PubMed: 11745036]

Forgac M. Structure, mechanism and regulation of the clathrin-coated vesicle and yeast vacuolar H(+)-ATPases. J Exp Biol. 2000; 203:71–80. [PubMed: 10600675]

Forgac M. Vacuolar ATPases: rotary proton pumps in physiology and pathophysiology. Nat Rev Mol Cell Biol. 2007; 8:917–29. [PubMed: 17912264]

Gissen P, Johnson CA, Morgan NV, Stapelbroek JM, Forshew T, Cooper WN, McKiernan PJ, Klomp LW, Morris AA, Wraith JE, McClean P, Lynch SA, Thompson RJ, Lo B, Quarrell OW, Di Rocco M, Trembath RC, Mandel H, Wali S, Karet FE, Knisely AS, Houwen RH, Kelly DA, Maher ER. Mutations in VPS33B, encoding a regulator of SNARE-dependent membrane fusion, cause arthrogryposis-renal dysfunction-cholestasis (ARC) syndrome. Nat Genet. 2004; 36:400–4. [PubMed: 15052268]

Gleizes PE, Munger JS, Nunes I, Harpel JG, Mazzieri R, Noguera I, Rifkin DB. TGF-beta latency: biological significance and mechanisms of activation. Stem Cells. 1997; 15:190–7. [PubMed: 9170210]

Gross JM, Perkins BD, Amsterdam A, Egana A, Darland T, Matsui JI, Sciascia S, Hopkins N, Dowling JE. Identification of zebrafish insertional mutants with defects in visual system development and function. Genetics. 2005; 170:245–61. [PubMed: 15716491]

Ho SY, Lorent K, Pack M, Farber SA. Zebrafish fat-free is required for intestinal lipid absorption and Golgi apparatus structure. Cell Metab. 2006; 3:289–300. [PubMed: 16581006]

Jan Danser AH, Batenburg WW, van Esch JH. Prorenin and the (pro)renin receptor--an update. Nephrol Dial Transplant. 2007; 22:1288–92. [PubMed: 17259648]

Kadesch T. Notch signaling: the demise of elegant simplicity. Curr Opin Genet Dev. 2004; 14:506–12. [PubMed: 15380241]

Kern G, Bosch ST, Unterhuber E, Pelster B. Mechanisms of acid secretion in pseudobranch cells of rainbow trout (Oncorhynchus mykiss). J Exp Biol. 2002; 205:2943–54. [PubMed: 12177159]

Kodama Y, Hijikata M, Kageyama R, Shimotohno K, Chiba T. The role of notch signaling in the development of intrahepatic bile ducts. Gastroenterology. 2004; 127:1775–86. [PubMed: 15578515]

Le Roy C, Wrana JL. Clathrin- and non-clathrin-mediated endocytic regulation of cell signalling. Nat Rev Mol Cell Biol. 2005; 6:112–26. [PubMed: 15687999]

Lemaigre F, Zaret KS. Liver development update: new embryo models, cell lineage control, and morphogenesis. Curr Opin Genet Dev. 2004; 14:582–90. [PubMed: 15380251]

Loomes KM, Russo P, Ryan M, Nelson A, Underkoffler L, Glover C, Fu H, Gridley T, Kaestner KH, Oakey RJ. Bile duct proliferation in liver-specific Jag1 conditional knockout mice: effects of gene dosage. Hepatology. 2007; 45:323–30. [PubMed: 17366661]

Lorent K, Moore JC, Siekmann AF, Lawson N, Pack M. Reiterative use of the notch signal during zebrafish intrahepatic biliary development. Dev Dyn. 2010; 239:855–64. [PubMed: 20108354]

Lorent K, Yeo SY, Oda T, Chandrasekharappa S, Chitnis A, Matthews RP, Pack M. Inhibition of Jagged-mediated Notch signaling disrupts zebrafish biliary development and generates multi-organ defects compatible with an Alagille syndrome phenocopy. Development. 2004; 131:5753–66. [PubMed: 15509774]

Lozier J, McCright B, Gridley T. Notch signaling regulates bile duct morphogenesis in mice. PLoS One. 2008; 3:e1851. [PubMed: 18365007]

Masuda H, Fukumoto M, Hirayoshi K, Nagata K. Coexpression of the collagen-binding stress protein HSP47 gene and the alpha 1(I) and alpha 1(III) collagen genes in carbon tetrachloride-induced rat liver fibrosis. J Clin Invest. 1994; 94:2481–8. [PubMed: 7989606]

Matthews RP, Eauclaire SF, Mugnier M, Lorent K, Cui S, Ross MM, Zhang Z, Russo P, Pack M. DNA hypomethylation causes bile duct defects in zebrafish and is a distinguishing feature of infantile biliary atresia. Hepatology. 2011

Matthews RP, Lorent K, Manoral-Mobias R, Huang Y, Gong W, Murray IV, Blair IA, Pack M. TNF{alpha}-dependent hepatic steatosis and liver degeneration caused by mutation of zebrafish s-adenosylhomocysteine hydrolase. Development. 2009; 136:865–75. [PubMed: 19201949]

Matthews RP, Lorent K, Pack M. Transcription factor onecut3 regulates intrahepatic biliary development in zebrafish. Dev Dyn. 2008; 237:124–31. [PubMed: 18095340]

Matthews RP, Lorent K, Russo P, Pack M. The zebrafish onecut gene hnf-6 functions in an evolutionarily conserved genetic pathway that regulates vertebrate biliary development. Dev Biol. 2004; 274:245–59. [PubMed: 15385156]

Matthews RP, Plumb-Rudewiez N, Lorent K, Gissen P, Johnson CA, Lemaigre F, Pack M. Zebrafish vps33b, an ortholog of the gene responsible for human arthrogryposis-renal dysfunction-cholestasis syndrome, regulates biliary development downstream of the onecut transcription factor hnf6. Development. 2005; 132:5295–306. [PubMed: 16284120]

Mellman I, Fuchs R, Helenius A. Acidification of the endocytic and exocytic pathways. Annu Rev Biochem. 1986; 55:663–700. [PubMed: 2874766]

Nakamura I, Sasaki T, Tanaka S, Takahashi N, Jimi E, Kurokawa T, Kita Y, Ihara S, Suda T, Fukui Y. Phosphatidylinositol-3 kinase is involved in ruffled border formation in osteoclasts. J Cell Physiol. 1997; 172:230–9. [PubMed: 9258344]

Navarro RE, Ramos-Balderas JL, Guerrero I, Pelcastre V, Maldonado E. Pigment dilution mutants from fish models with connection to lysosome-related organelles and vesicular traffic genes. Zebrafish. 2008; 5:309–18. [PubMed: 19133829]

Nguyen G, Delarue F, Burckle C, Bouzhir L, Giller T, Sraer JD. Pivotal role of the renin/prorenin receptor in angiotensin II production and cellular responses to renin. J Clin Invest. 2002; 109:1417–27. [PubMed: 12045255]

Nichols JT, Miyamoto A, Weinmaster G. Notch signaling--constantly on the move. Traffic. 2007; 8:959–69. [PubMed: 17547700]

Nickerson DP, Brett CL, Merz AJ. Vps-C complexes: gatekeepers of endolysosomal traffic. Curr Opin Cell Biol. 2009; 21:543–51. [PubMed: 19577915]

Oka T, Krieger M. Multi-component protein complexes and Golgi membrane trafficking. J Biochem. 2005; 137:109–14. [PubMed: 15749823]

Pack M, Solnica-Krezel L, Malicki J, Neuhauss SC, Schier AF, Stemple DL, Driever W, Fishman MC. Mutations affecting development of zebrafish digestive organs. Development. 1996; 123:321–8. [PubMed: 9007252]

Pickart MA, Sivasubbu S, Nielsen AL, Shriram S, King RA, Ekker SC. Functional genomics tools for the analysis of zebrafish pigment. Pigment Cell Res. 2004; 17:461–70. [PubMed: 15357832]

Roth-Eichhorn S, Kuhl K, Gressner AM. Subcellular localization of (latent) transforming growth factor beta and the latent TGF-beta binding protein in rat hepatocytes and hepatic stellate cells. Hepatology. 1998; 28:1588–96. [PubMed: 9828223]

Ryan MJ, Bales C, Nelson A, Gonzalez DM, Underkoffler L, Segalov M, Wilson-Rawls J, Cole SE, Moran JL, Russo P, Spinner NB, Kusumi K, Loomes KM. Bile duct proliferation in Jag1/fringe heterozygous mice identifies candidate modifiers of the Alagille syndrome hepatic phenotype. Hepatology. 2008; 48:1989–97. [PubMed: 19026002]

Sadler KC, Amsterdam A, Soroka C, Boyer J, Hopkins N. A genetic screen in zebrafish identifies the mutants vps18, nf2 and foie gras as models of liver disease. Development. 2005; 132:3561–72. [PubMed: 16000385]

Saroussi S, Nelson N. Vacuolar H(+)-ATPase-an enzyme for all seasons. Pflugers Arch. 2008

Schefe JH, Menk M, Reinemund J, Effertz K, Hobbs RM, Pandolfi PP, Ruiz P, Unger T, Funke-Kaiser H. A novel signal transduction cascade involving direct physical interaction of the renin/prorenin receptor with the transcription factor promyelocytic zinc finger protein. Circ Res. 2006; 99:1355–66. [PubMed: 17082479]

Schonthaler HB, Fleisch VC, Biehlmaier O, Makhankov Y, Rinner O, Bahadori R, Geisler R, Schwarz H, Neuhauss SC, Dahm R. The zebrafish mutant lbk/vam6 resembles human multisystemic disorders caused by aberrant trafficking of endosomal vesicles. Development. 2008; 135:387–99. [PubMed: 18077594]

Sun-Wada GH, Wada Y, Futai M. Diverse and essential roles of mammalian vacuolar-type proton pump ATPase: toward the physiological understanding of inside acidic compartments. Biochim Biophys Acta. 2004; 1658:106–14. [PubMed: 15282181]

Toei M, Saum R, Forgac M. Regulation and isoform function of the V-ATPases. Biochemistry. 2010; 49:4715–23. [PubMed: 20450191]

Wagner DS, Dosch R, Mintzer KA, Wiemelt AP, Mullins MC. Maternal control of development at the midblastula transition and beyond: mutants from the zebrafish II. Dev Cell. 2004; 6:781–90. [PubMed: 15177027]

Wang H, Kesinger JW, Zhou Q, Wren JD, Martin G, Turner S, Tang Y, Frank MB, Centola M. Identification and characterization of zebrafish ocular formation genes. Genome. 2008; 51:222–35. [PubMed: 18356958]

Westerfield, M. The zebrafish book. A guide for the laboratory use of zebrafish (Danio rerio). University of Oregon Press; Eugene: 2000.

Yan Y, Denef N, Schupbach T. The vacuolar proton pump, V-ATPase, is required for notch signaling and endosomal trafficking in Drosophila. Dev Cell. 2009; 17:387–402. [PubMed: 19758563]

Yee NS, Lorent K, Pack M. Exocrine pancreas development in zebrafish. Dev Biol. 2005; 284:84–101. [PubMed: 15963491]

Zong Y, Panikkar A, Xu J, Antoniou A, Raynaud P, Lemaigre F, Stanger BZ. Notch signaling controls liver development by regulating biliary differentiation. Development. 2009; 136:1727–39. [PubMed: 19369401]

Highlights

- We report the identification of three novel zebrafish biliary mutants
- One of these mutants, *pekin*, is caused by a mutation in the vacuolar H^+-ATPase subunit gene *atp6ap2*
- *Pekin* also demonstrates hypopigmentation and defects in pancreas and intestine
- Other V-H^+-ATPase mutants also demonstrate biliary defects, and genetic inhibition of *atp6ap2* and other trafficking genes is additive, supporting an important role for trafficking pathways in biliary development.

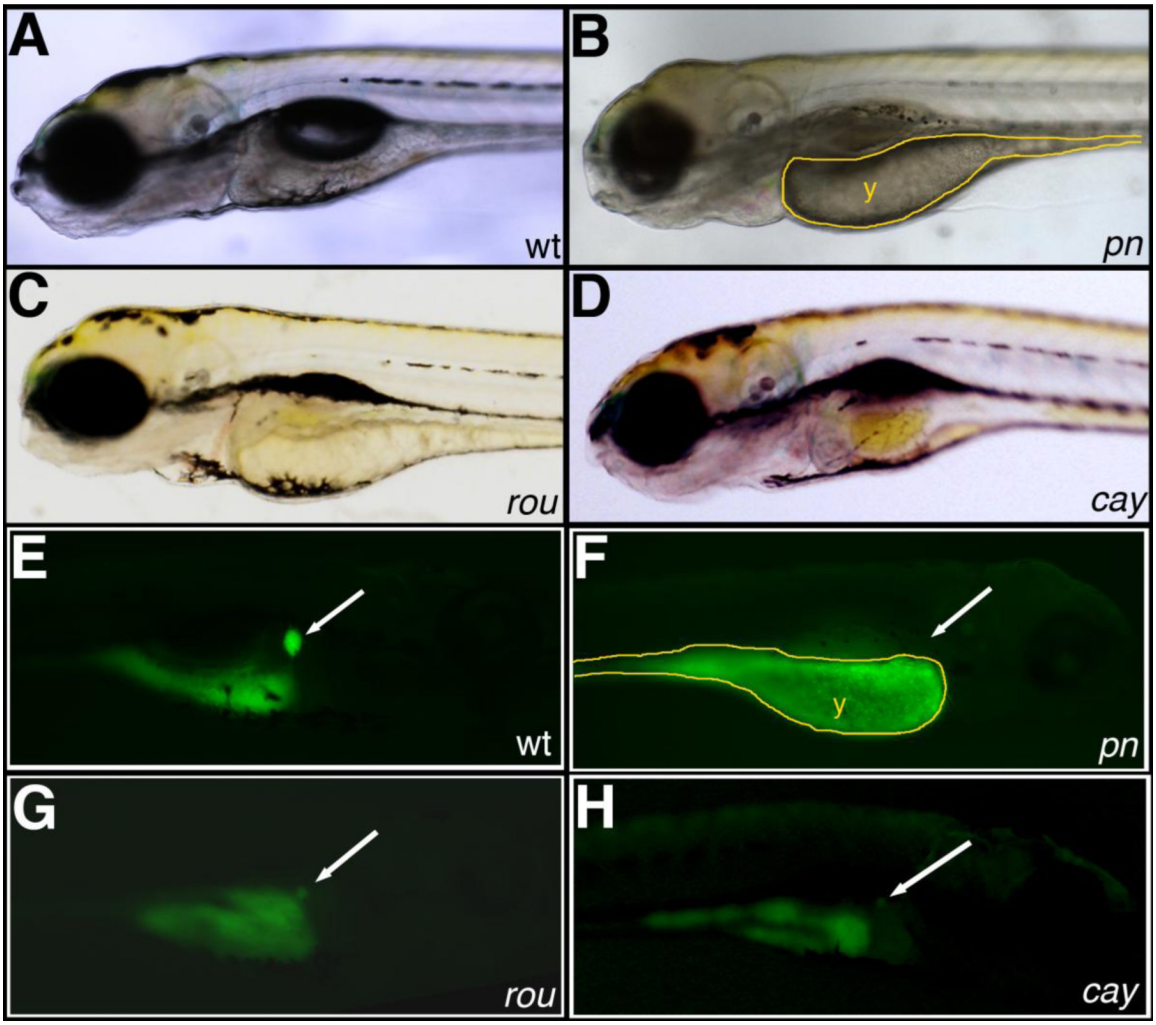

Figure 1. Novel mutants with abnormal PED-6 uptake

(A-D) Left lateral views of live 5 dpf wild-type (A, wt), *pekin* (B, *pn*), *rouen* (C, *rou*), and *cayuga* (D, *cay*) larvae. *pn* demonstrates global hypopigmentation, underutilized yolk (y), absent swim bladder and some brain edema. (E-H) Right lateral views of the same 5 dpf larvae after PED-6 uptake, demonstrating normal intensity of the gallbladder in wt (E, white arrow), but absent gallbladders in the mutants (F-H, white arrows).

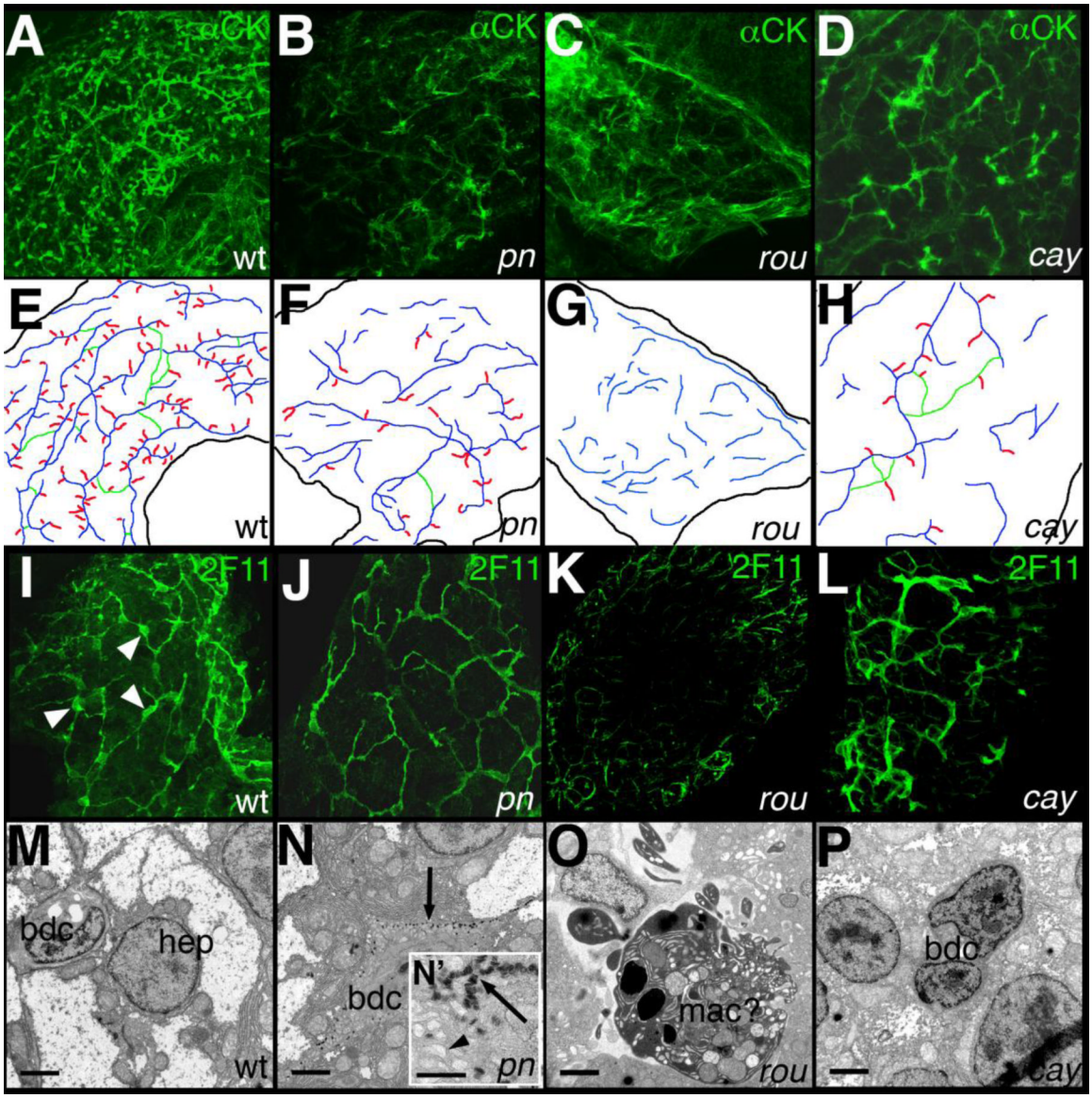

Figure 2. Intrahepatic biliary defects in novel mutants

(A-D) Confocal projections of whole-mount cytokeratin immunostaining of livers from 5 dpf wild-type (A, wt), *pekin* (B, *pn*), *rouen* (C, *rou*), and *cayuga* (D, *cay*) larvae, schematized in (E-H). The typical wt pattern is depicted in (A) and schematized in (E), demonstrating a complex latticework. In contrast, the staining pattern of *pn* (B, F) demonstrates shorter ducts with fewer interconnections. The staining pattern of *rou* (C, G) demonstrates an absence of recognizable ducts. The cytokeratin staining pattern of *cay* (D, H) demonstrates short non-interconnected ducts, with some terminal ductules. (I-L) Confocal projections of whole-mount 2F11 immunostaining of livers from 5 dpf wt (I), *pn* (J), *rou* (K), and *cay* (L) larvae. 2F11 stains bile duct cell bodies (white arrowheads) and proximal ducts, as demonstrated in wt (I). The 2F11 pattern of *pn* demonstrates fewer ducts, with smaller bile duct cells. There are no apparent bile duct cells in 2F11 stainings of *rou* (K), and *cay* (L) is similar to wt. (M-P) Electron micrographs of livers from 5 dpf wt (M), *pn* (N), *rou* (O), and *cay* (O) larvae. In (M), the wt hepatocyte (hep) and bile duct cell (bdc) are depicted. In contrast, the bdc in *pn* (N) contains an accumulation of electron dense material

(black arrow) at the periphery of the cell. The inset (N') demonstrates that these bodies have a striped appearance, and the dilated vesicles (black arrowhead) are also apparent. The cell in *rou* (O) is most likely a macrophage (mac), in the space normally occupied by bile duct cells. In contrast, the bdc of *cay* (P) appears close to normal, but with nuclei that are modestly enlarged relative to the cytoplasm when compared to wt (M), and with an appearance more closely resembling the hep nucleus. Scale bars in (M-P) 500 nm, N' also 500 nm.

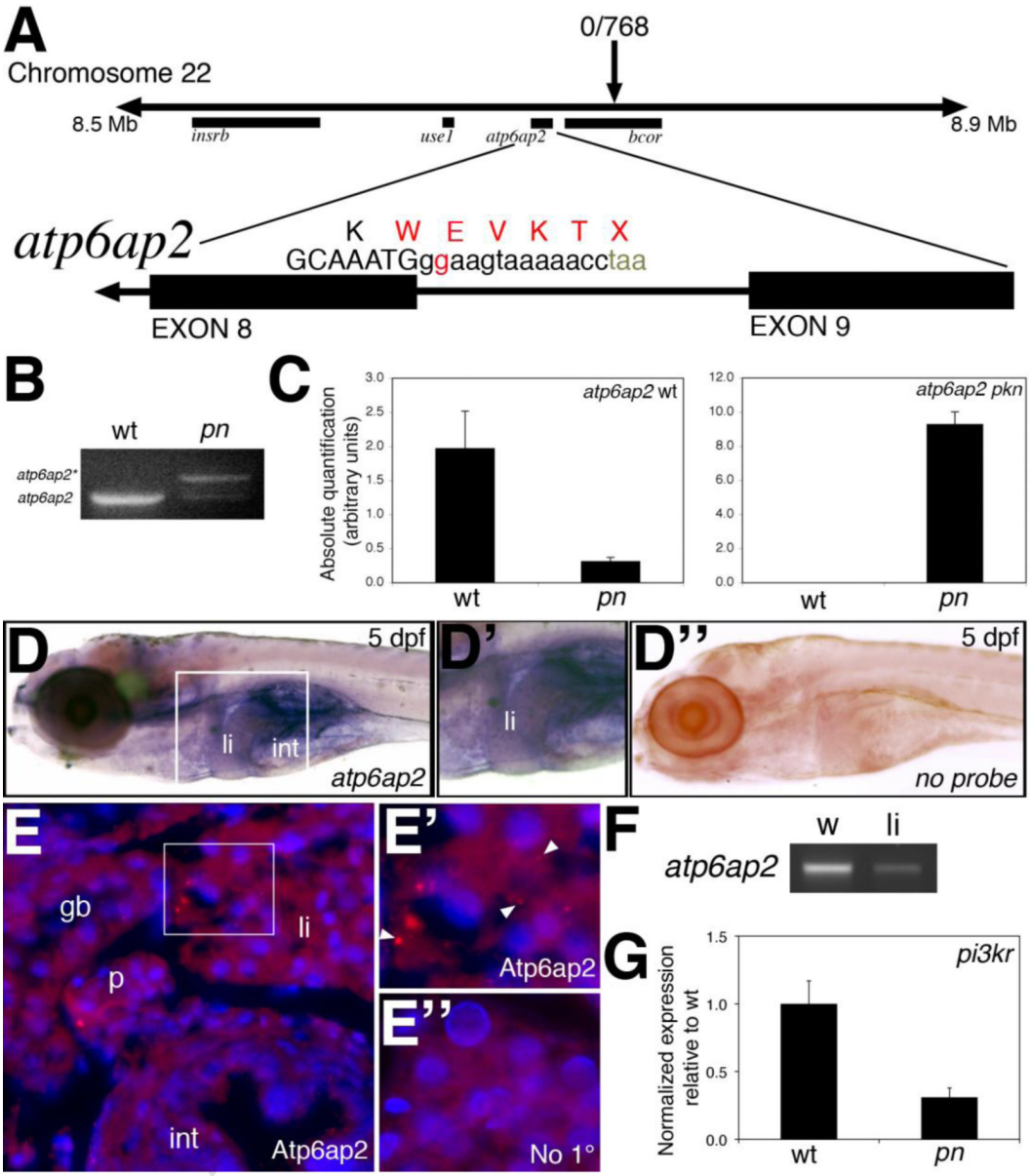

Figure 3. Mapping and genetic characterization of *pn*

(A) Schematic of mapping around the *pn* locus. A region of interest on chromosome 22 was identified as depicted, with a zero recombinant marker in the *bcor* gene. A splice donor site mutation following exon 8 of *atp6ap2* was detected in *pn* mutants, which would result in the depicted sequence. (B) PCR of the wild-type (wt) and *pn* splice products, demonstrating the presence of the higher band (*atp6ap2**), corresponding to the read-through product. (C) Quantitative PCR of the wt and *pn atp6ap2* splice products, demonstrating a 10x reduction in the wt product in *pn*, and a very large increase in the amount of the mutant transcript in *pn*. (D) *In situ* hybridization of *atp6ap2* at 5 dpf demonstrates liver ("li") and intestinal ("int") expression of *atp6ap2*, shown in higher magnification in D'. Compare to (D''), which is a similarly processed 5 dpf larva without *atp6ap2* riboprobe, with no specific staining. (E) Immunostaining of Atp6ap2 in 5 dpf cross-sections demonstrates staining in liver ("li"), intestine ("int"), pancreas ("p"), and gallbladder ("gb"). The area within the white rectangle is shown in E', demonstrating punctate staining (white arrowheads), consistent with a

vesicular localization, within the liver. (E'') Liver section from a 5 dpf larva processed similarly but without primary antibody, at the same magnification as (E'), showing no punctate staining. (E), (E') and (E'') are counterstained with DAPI to show nuclei. (F) PCR of *atp6ap2* from 5 dpf whole larvae (w) and from livers (li) isolated from 5 dpf larvae, showing expression of *atp6ap2*. (G) Quantitative PCR demonstrating a 5x decrease in *pi3kr1* expression, a gene regulated by Atp6ap2 via PLZF.

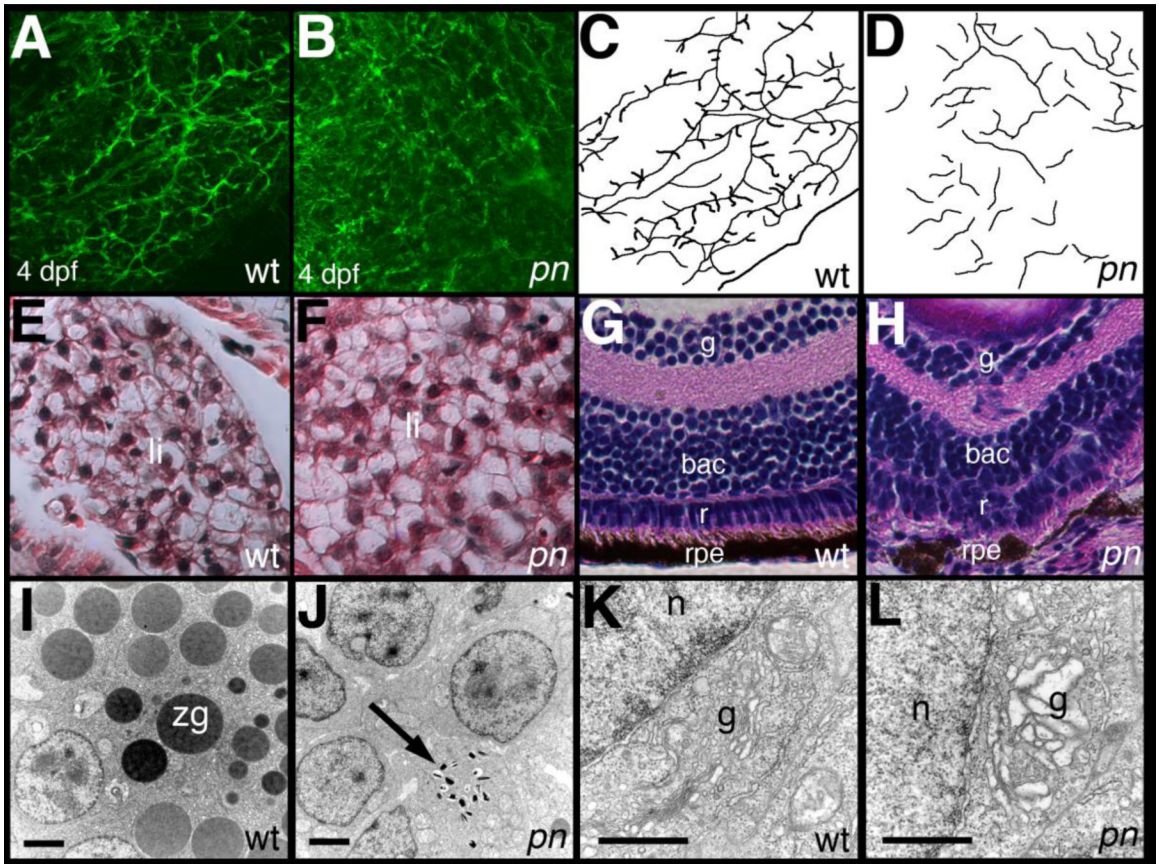

Figure 4. Additional defects in *pn* larvae

(A-D) Confocal projections of whole-mount cytokeratin immunostaining of livers from 4 dpf wild-type (A, wt) and *pekin* (B, *pn*) larvae, demonstrating abnormalities at this earlier stage. Ducts are short and demonstrate few if any connections. These abnormalities are schematized in (C-D). (E-F) Hematoxylin and eosin staining of cross-sections of 5 dpf wt (E) and *pn* (F) larvae, demonstrating that at this resolution the liver of a *pn* larva appears normal. (G-H) Hematoxylin and eosin staining of the eye from a 5 dpf wt (G) and *pn* (H) larva. Note the ordered appearance of the cell layers in the wt eye, including the inner ganglionic (ig), outer ganglionic (og), retinal (r), and retinal pigmented epithelial (rpe) layers. In contrast, cells in these layers are disordered in *pn*, in particular in the retinal layer, which is difficult to distinguish from the og layer. The rpe is also poorly formed in *pn*. (I-L) Electron micrographs of pancreas (I-J) and enterocytes (K-L) from wt (I, K) and *pn* (J, L). Note the presence of numerous zymogen granules (zg) in wt pancreas are absent in*pn*, although there are small structures that may represent poorly formed zg (black arrow). The Golgi (g) in the *pn* enterocyte (L) appears dilated relative to the Golgi of wt (K). n, nucleus. Scale bars 500 nm.

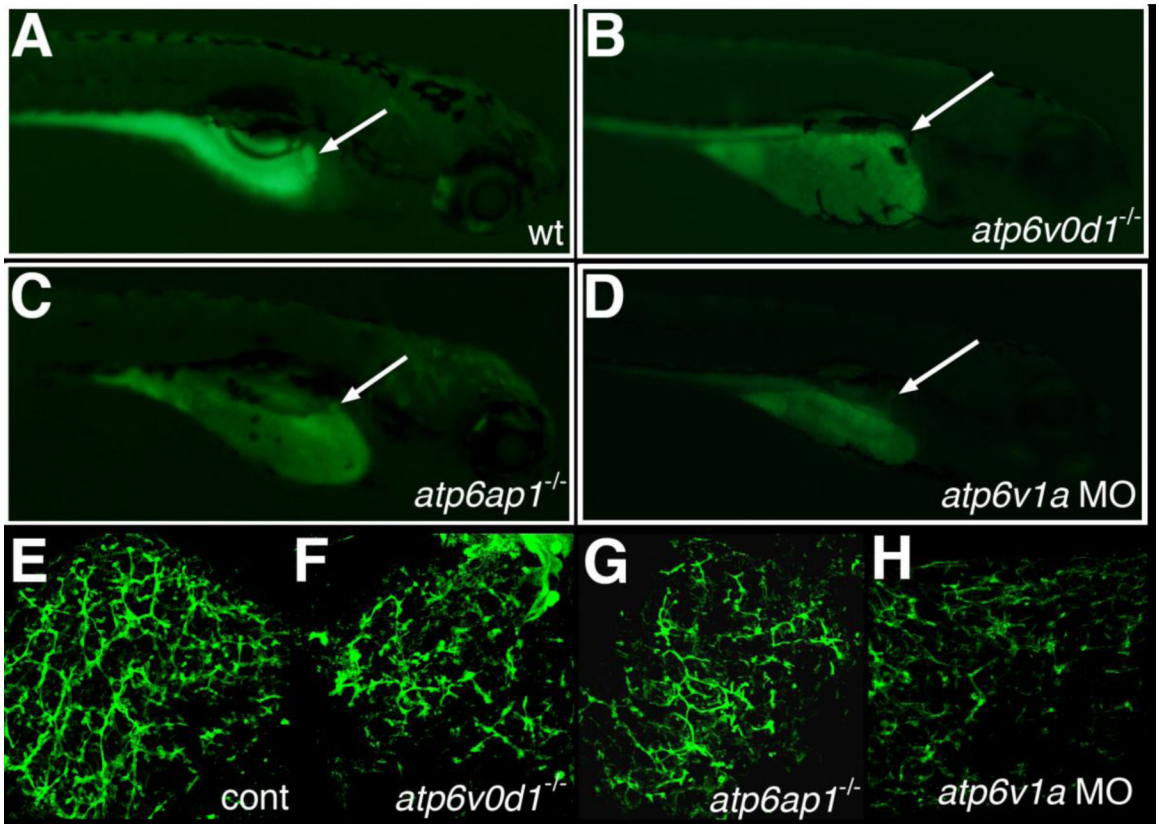

Figure 5. Intrahepatic biliary defects in other V-H$^+$-ATPase mutants

(A-D) Right lateral views of 5 dpf larvae after administration of the fluorescent lipid reporter PED-6. (A) Control larva demonstrates normal gallbladder intensity (white arrow). (B) 5 dpf *atp6v0d1*$^{-/-}$ mutant, (C) 5 dpf *atp6ap1*$^{-/-}$ mutant, and (D) 5 dpf *atp6v1a* morpholino (MO)-injected larvae all demonstrate a decrease or lack of gallbladder fluorescence (white arrows). (E-H) Confocal projections of cytokeratin immunostaining of 5 dpf liver from control (E), *atp6v0d1*$^{-/-}$, *atp6ap1*$^{-/-}$, and *atp6v1a* MO-injected larvae. The abnormal cytokeratin pattern in (F-H) has similarities to the pattern noted in *pn*, with fewer ducts overall and focal areas of ectatic ducts.

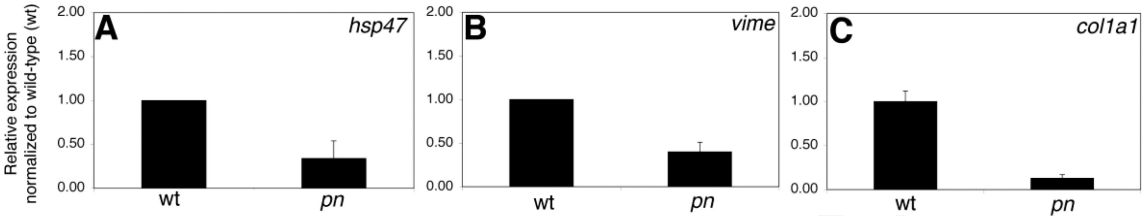

Figure 6. Changes in fibrogenic gene expression in *pn*

Quantitative real-time PCR on *pn* for *hsp47* (A), *vimentin* (*vime*) (B), and collagen I(α)I (*col1a1*) (C). There is a significant decrease ($p<0.03$, $p<0.05$, $p<0.01$) for all three genes. QPCR results for the other V-H^+-ATPase gene mutants and morphants show minimal changes and are depicted in supplemental Figure 5.

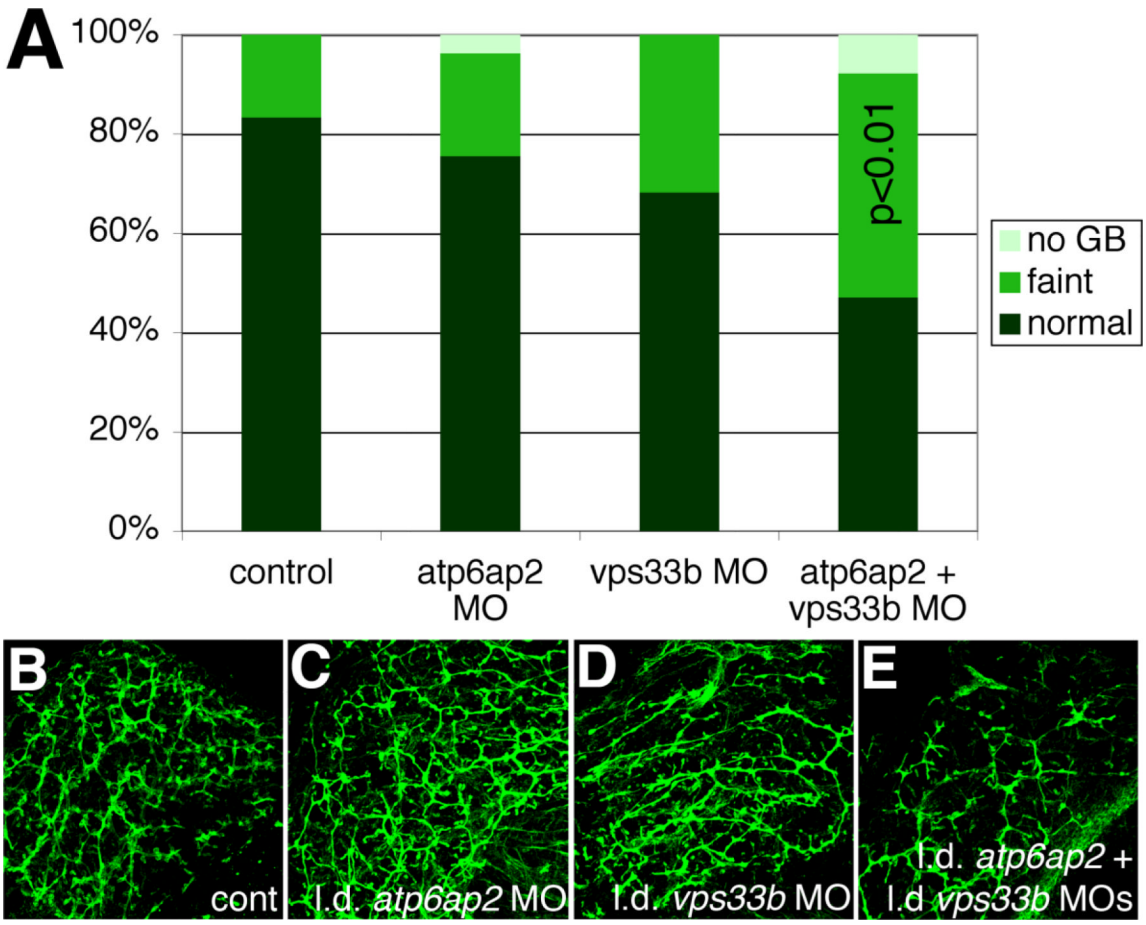

Figure 7. Additive effect of *vps33b* and *atp6ap2* inhibition

(A) Gallbladder PED-6 uptake in 5 dpf control larvae (cont), larvae injected with a low dose of *atp6ap2* morpholino (MO), larvae injected with a low dose of *vps33b* MO, and larvae injected with a combination of the low dose MOs. The number of larvae with faint gallbladders was not significantly different between either of the MOs alone compared to control, but the number of larvae with faint gallbladders after injection of the combination of MOs was significantly increased compared to control ($p<0.01$) and to either of the MOs alone ($p<0.01$ for *atp6ap2*, $p<0.05$ for *vps33b*). (B-E) Confocal projections of cytokeratin immunostaining from 5 dpf larvae corresponding to the conditions depicted in the graph in (B), showing control (B, cont), low-dose *atp6ap2* MO (C), low-dose *vps33b* MO (D), and the combination of the two MOs in low dose (E). Note that (C) and (D) are similar to (B), while (E) more closely resembles the *pn* defects shown above. Samples depicted in B-E are representative of pooled samples of all PED-6 classifications.

Table 1

Quantification of duct characteristics of mutants and morphants.

	# total ducts	# int. ducts	# terminal ductules	length	width	angle
wt	37.3±9.8	13.5±6.2	93.8±23.5	1.55±0.15	0.320±0.051	73±10
pekin	49.2±20.6	1.2±1.2**	35.3±28.5**	0.97±0.14***	0.457±0.113*	70±7
rouen	13.3±2.0***	1.3±1.0**	0.2±0.4***	0.87±0.21***	0.559±0.077***	82±16
cayuga	17.2±6.5**	1.6±1.3**	9.6±7.7***	1.64±0.33	0.478±0.075**	86±10
atp6ap1$^{-/-}$	48.7±6.4	4.3±0.6*	39.7±19.4*	1.07±0.30*	0.356±0.038	76±13
atp6v0d1$^{-/-}$	29.5±16.3	0.0±0.0**	6.0±5.7**	0.72±0.12***	0.325±0.025	76±25
atp6v1a MO	50.0±3.6	3.0±1.0*	24.0±8.7**	0.97±0.19***	0.351±0.048	79±14
atp6ap2 MO	35.0±7.8	0.8±0.5**	32.3±8.3**	1.01±0.09***	0.434±0.048*	79±7

Shown are average number of total ducts, interconnecting ducts (IC), and terminal ductules, duct length, width, and angle. N=6 samples per condition for wt, pekin, rouen, and cayuga; N=3 for *atp6ap1*$^{-/-}$, *atp6v0d1*$^{-/-}$, *atp6v1a* MO and *atp6ap2* MO.

* p≤0.05

** p≤0.005

*** p≤0.0005.